

Independent Approximates provide a maximum likelihood estimate for heavy-tailed distributions

Amenah Al-Najafi^{1,*}, Ugur Tirnakli² and Kenric P. Nelson³

¹Department of Mathematics, University of Kufa, 299G, Najaf, Iraq.

²Department of Physics, Faculty of Arts and Sciences, Izmir University of Economics, 35330, Izmir, Turkey.

³Photrek, LLC, 56 Burnham St Unit 1, Watertown, MA, USA.

*Corresponding author(s). E-mail(s): amenah.alnajafi@gmail.com;
Contributing authors: ugur.tirnakli@ieu.edu.tr; kenric.nelson@photrek.io;

Abstract

Heavy-tailed distributions are infamously difficult to estimate because their moments tend to infinity as the shape of the tail decay increases. Nevertheless, this study shows the utilization of a modified group of moments for estimating a heavy-tailed distribution. These modified moments are determined from powers of the original distribution. The n th-power distribution is guaranteed to have finite moments up to $n - 1$. Samples from the n th-power distribution are drawn from n -tuple Independent Approximates, which are the set of independent samples grouped into n -tuples and sub-selected to be approximately equal to each other. We show that Independent Approximates are a maximum likelihood estimator for the generalized Pareto and the Student's t distributions, which are members of the family of coupled exponential distributions. We use the first (original), second, and third power distributions to estimate their zeroth (geometric mean), first, and second power-moments respectively. In turn, these power-moments are used to estimate the scale and shape of the distributions. A least absolute deviation criteria is used to select the optimal set of Independent Approximates. Estimates using higher powers and moments are possible though the number of n -tuples that are approximately equal may be limited.

Keywords: Independent Approximate, coupled exponential, coupled Gaussian, least absolute deviation

1 Introduction

Heavy-tailed distributions play a crucial role in characterizing the statistics of complex systems and find applications in various fields, including finance, climatology, telecommunication, genetics, and more [Resnick \(2007\)](#), [Merz et al. \(2022\)](#), [Ibragimov et al. \(2015\)](#) and [Bradley and Taqqu \(2003\)](#). These distributions possess tails that decay slower than the exponential distribution, making their estimation challenging but essential for diverse scientific and engineering studies. Several tail index estimators have been proposed in the literature, including Hill’s estimator (1975), Pickand’s estimator (1975), and Dekker’s et al. (1989). While these estimators play a fundamental role in diverse scientific and engineering studies by addressing distributions with tails that decay slower than the exponential distribution, they are not without challenges. Since the estimator depends on the number of upper order statistics k , determining the optimal number poses a challenge. Moreover, the sensitivity of the estimate to the choice of k further complicates the selection process.

The statistical mechanics of complex systems has been advanced by the methods of nonextensive statistical mechanics (NSM) introduced by Tsallis [Tsallis \(2017\)](#). Convergence to heavy-tailed distributions for nonlinear systems has been shown via maximization of a generalized entropy function and through a generalized central limit theorem [Umarov et al. \(2008\)](#); [Umarov and Tsallis \(2016\)](#). The family of Tsallis q -probability density functions is defined as $f(x; q, \beta, \alpha) = \frac{1}{Z_q(\beta, \alpha)} [1 + (1 - q)\beta x^\alpha]^{1/(1-q)}$ where $\alpha = 1$ is the q -exponential distribution and $\alpha = 2$ is the q -Gaussian distribution. Shalizi [Shalizi \(2007\)](#) established a maximum likelihood estimator for the q -exponential distribution, which is equivalent to the Generalized Pareto Distribution. One of the authors (Nelson) introduced an approach to NSM, known as Nonlinear Statistical Coupling (NSC), that isolates three independent parameters embedded within the parameter q . The nonlinear statistical coupling or coupling for short, κ , is isolated if the dimensions, d , and the power of the variable, α , are separated. The coupled exponential distribution (equivalent to q -exponential or GPD) has $\alpha = 1$ and the coupled Gaussian (equivalent to q -Gaussian or Student’s t) has $\alpha = 2$. The family of coupled exponential distributions is defined in the next section.

In this paper, we evaluate the performance of the IA method, introduced by one of the authors, Nelson [Nelson \(2022\)](#). IAs facilitate the estimation of heavy-tailed distributions via a filtering process that selects subsamples with a distribution that has faster-decaying tails while preserving a functional relationship with the distribution of the original samples. We demonstrate that pairs and triplets of IAs ensure that the first and second moments are defined respectively for all heavy-tailed members of the coupled distribution family, $\kappa > 0$. Utilizing the least absolute deviations (LAD), we obtain the optimal subsample set for statistical analysis. We assess the performance of our estimators using Coefficient of Efficiency, Average Deviation (AD), Cramer–von Mises (CvM), and Negative Log-Likelihood (NLL) as criteria under different underlying estimators.

2 The Coupled Distribution Family

We will examine the performance of the IA estimator for the generalized Pareto and the Student's t distributions. To facilitate the discussion we define the family of *coupled distributions* which includes the Pareto and Student's t. The coupling, κ , refers to the degree of nonlinear coupling deviating from the exponential and logarithm functions of linear analysis, and parameterizes the generalizations, $\exp_{\kappa} x \equiv (1 + \kappa) \frac{x}{\sigma}$; $(a)_{+} = \max(0, a)$ and $\ln_{\kappa} x \equiv \frac{1}{\kappa} (x^{\kappa} - 1)$; $x > 0$. The reciprocal of the generalized exponential function is the survival function (SF) (1 - the cumulative distribution function (CDF)) of generalized Pareto distribution, $S(x; \mu, \sigma, \kappa) = 1 - F(x; \mu, \sigma, \kappa) \equiv (\exp_{\kappa}(\frac{x-\mu}{\sigma}))^{-1}$. The family of coupled distributions is defined to preserve the role of the coupling as the shape parameter of the distributions, heavy-tailed for $\kappa > 0$; exponential for $\kappa = 0$; and compact-support for $\kappa < 0$. The connection with the Student's t distribution establishes the coupling as the reciprocal of the degree of freedom. Given the relationship between nonlinear systems and complexity, the coupling can also serve as a measure of statistical complexity.

The coupled distribution is defined such that the power α of the variable x is one for the generalized Pareto distribution and two for the Student's t distribution. The symmetric two-sided version of the coupled CDF, like the Student's t CDF, is a function of the regularized incomplete beta function, $I(z; a, b)$

$$F(x; \mu, \sigma, \kappa, \alpha) \equiv \begin{cases} \frac{1}{2} I\left(\frac{1}{1+\kappa} \left|\frac{x-\mu}{\sigma}\right|^{\alpha}, \frac{1}{\alpha\kappa}, \frac{1}{\alpha}\right) & x \leq \mu \\ \frac{1}{2} + \frac{1}{2} I\left(\frac{\kappa}{1+\kappa} \left|\frac{x-\mu}{\sigma}\right|^{\alpha}, \frac{1}{\alpha}, \frac{1}{\alpha\kappa}\right) & \text{True} \end{cases} \quad (1)$$

The two-sided coupled PDF is defined as

$$f(x; \mu, \sigma, \kappa, \alpha) \equiv \begin{cases} \frac{1}{Z(\sigma, \kappa, \alpha)} \left(1 + \kappa \left|\frac{x-\mu}{\sigma}\right|^{\alpha}\right)^{-\frac{1+\kappa}{\alpha\kappa}} & \kappa \neq 0 \\ \frac{1}{Z(\sigma, \alpha)} \exp\left(-\frac{1}{\alpha} \left|\frac{x-\mu}{\sigma}\right|^{\alpha}\right) & \kappa = 0 \end{cases}, \sigma \geq 0, -1 \leq \kappa, 0 < \alpha < 2 \quad (2)$$

where the generalized Pareto ((coupled exponential) distribution is $\alpha = 1$ and the Student's t (coupled Gaussian) distribution is $\alpha = 2$. The normalization or partition function, Z , is

$$Z(\sigma, \kappa, \alpha) \equiv \begin{cases} \sigma & \alpha = 1 \\ \frac{\sigma B\left(\frac{1}{2\kappa}, \frac{1}{2}\right)}{\sqrt{\kappa}} & \kappa > 0 \\ \sigma\sqrt{2\pi} & \kappa = 0 \\ \frac{\sigma B\left(\frac{-1+\kappa}{2\kappa}, \frac{1}{2}\right)}{\sqrt{-\kappa}} & -1 \leq \kappa < 0 \end{cases} \quad (3)$$

where B is the (incomplete, $z \neq 1$) Beta function, $B(z, a, b) = \int_0^z t^{a-1} (1-t)^{b-1} dt$ and the regularized incomplete beta function is $I(z; a, b) = \frac{B(z; a, b)}{B(a, b)}$. σ is the scale of the distribution and equals the standard deviation when $\kappa = 0$. The scale of the coupled distribution is at the knee of the log-log plot of the PDF. On the log-log plot the PDF has zero slope at $x = \mu$, and a slope of $-\frac{1+\kappa}{\alpha}$ for $x \rightarrow \infty$. At $x = \sigma$ the

log-log slope is -1 for all values of κ and α . Also, at $x = -\frac{\sigma}{\kappa\alpha}$ the slope is half the value at infinity, $-\frac{1+\kappa}{2\kappa}$ and the second derivative is a maximum. These properties are reviewed further in Appendix A. The clarity of mathematical definitions for the scale, shape, and power of the variable for the coupled distribution will facilitate physical interpretations of the statistical properties of complex systems. The relationship with the Tsallis parameter q is determined by the exponent of the distribution,

$$q = 1 + \frac{\alpha\kappa}{1 + \kappa}; \quad \kappa = \frac{q - 1}{\alpha - q + 1}. \quad (4)$$

The relationship with β is determined by the term multiplying x ,

$$\beta = \frac{1 + \kappa}{\alpha\sigma^\alpha}; \quad \sigma = \left(\frac{q - 1}{\beta(q - 1)(\alpha + 1 - q)} \right)^{\frac{1}{\alpha}}. \quad (5)$$

3 Estimation using Independent Approximates

In this paper, we analyze the performance of estimation using Independent Approximates Nelson (2022), in which independent samples from a random variable $X \sim f(x)$ are split into n -dimensions for subsampling of n -tuplets that are approximately equal. Our theoretical analysis assumes samples that are on the equal marginal of the n -dimensional distribution of X . These are referred to as "Independent-Equals" and are symbolically represented as $X^{(n)} \sim f^{(n)}(x) = \frac{f^n(x)}{\int_{x \in X} f^n(x)}$.

Our experimental approach entails selects samples from a tolerance neighborhood ϵ around the independent equals marginal distribution, which we term Independent-Approximates (IAs), denoted as $X^{(n)} \sim \hat{f}^{(n)}(x)$. The idea behind selecting these Independent Approximate samples is to obtain a subset of the data that has a lower shape parameter and thus has moments that can be estimated but retains a functional relationship with the original distribution's parameters.

In the case of the coupled distribution family, we specifically focus on the IA method when the shape parameter α is 1 or 2. We create estimators for the n th power of a density by taking N independent and identically distributed samples and dividing them into subsets of length n . The subsets that have absolute values approximately equal are then selected. The median of these selected subsets gives us a set of Independent Approximates (IA) of size $N^{(n)} \equiv \lfloor (N/n) \rfloor$.

Definition 1 (Power-moment). *The m th moment of the n th power of density $f_X(x)$ function defined as*

$$\mu_m^{(n)} = \frac{\int_{x \in X} x^m f_X^n(x) dx}{\int_{x \in X} f_X^n(x) dx} = E[(X^{(n)})^m].$$

To illustrate the concept of the m th moment of the n th power density, let's consider the zeroth moment. In this scenario, we can define $f^{(n)}(x)$ as

$$f^{(n)} = \frac{f^n(x)}{\int_{x \in X} f^n(x)}$$

The above expression represents the density of the marginal distribution along the diagonal of n equal values when the m th moment is zero.

The concept of power-density moments allows for a mapping between estimates that can be obtained from the reduced shape of a distribution and those of the original distribution. If a distribution is raised to the power of $(m + 1)$ and renormalized, then the m th moment exists and is finite for all shapes ($\kappa \geq 0$), Nelson (2022). Table 1 provides the functional relationship between moments and the n th power of the generalized Pareto distribution, considering the location, scale, and shape parameters.

In the subsequent sections, we delve into the application and analysis of the IA method for the coupled distribution family, with a specific focus on the cases where α is 1 or 2.

3.1 Selecting independent approximate subsamples (IAs)

Our approach builds upon Nelson's IA method Nelson (2022), introducing a more general class of estimators and applying the least absolute deviation (LAD) to carefully select the optimal subsample. The algorithm is detailed below, providing a comprehensive understanding of our approach. Use of the LAD enhances the robustness and applicability of the IA method. Let X_1, X_2, \dots, X_N be independent, identically distributed samples from a one-dimensional random variable with a one dimensional distribution $X_i \sim F(x)$. We randomly partition the samples into $n - \text{tuple}$ groups, so there are $I = \lfloor N/n \rfloor$ groups denoted by $(X_{i_1}, X_{i_2}, \dots, X_{i_n}), (X_{i_{n+1}}, X_{i_{n+2}}, \dots, X_{i_{2n}}), \dots, (X_{i_{(n \cdot I) - (n-1)}}, X_{i_{(n \cdot I) - (n-2)}}, \dots, X_{i_N})$, where i_1, i_2, \dots, i_N is a random permutation of the integers $1, 2, \dots, N$. Let \mathcal{D} be the set of all absolute differences calculated for each group as $d_n = \max(X_{i_j}^{(n)}) - \min(X_{i_{j+1}}^{(n)})$. Since the samples X_1, X_2, \dots, X_N are independently and identically distributed, the elements in \mathcal{D} will be randomly distributed. Now, we sort the elements in \mathcal{D} in ascending order, denoted by $\mathcal{D}_{\text{sorted}}$, such that $d_1 \leq d_2 \leq \dots \leq d_N$. Thus the Independent Approximate is

$$IAs =: \{d_i \in \mathcal{D}_{\text{sorted}} | d_i \leq \varepsilon\}$$

Then, we select the median M_n of each I -tuple as the subsample, i.e., $M_n = \text{Median}(X_{i_1}, X_{i_2}, \dots, X_{i_n})$ for $(X_{i_1}, X_{i_2}, \dots, X_{i_n}) \in IAs$. In this study, the threshold ε is not predefined but is instead determined dynamically by the algorithm during the data processing. The algorithm starts by considering pairs with the smallest absolute differences and gradually increases the threshold until it finds the appropriate limit that yields the best result. The selection of the optimal threshold relies on minimizing the least absolute deviation. This ordering of the absolute deviation is similar to the order statistics analysis used in the Hill estimator for the shape.

In order to estimate the parameters of the heavy tail distribution, we consider X_1, X_2, \dots, X_N independent identically distribution (*iid*) drawn from a coupled distribution, with α either 1 or 2, where N denotes the sample size. We use 25 permutations to select the independent approximate samples (IAs). Under the assumption that $\mu = 0$, the (IAs) and the optimal number of sub-samples are selected as:

1. If estimating scale:
 - (a) Partition the samples randomly into pairs and select equal pairs using $d_k = \{(X_{i_{2I-1}}^{(2)} - X_{i_{2I}}^{(2)}) : I = 1, 2, \dots, \lfloor N/2 \rfloor, |X_{i_{2I-1}}^{(2)} - X_{i_{2I}}^{(2)}|\}$, sort the pairs by their distance.
 - (b) Find the median of these pairs M_I to form a vector of independent approximation (IA) $M_I = \text{Median}\{X_{i_{2I-1}}, X_{i_{2I}}\}$ for $(X_{i_{2I-1}}, X_{i_{2I}} \in d_I)$.
 - (c) To determine the optimal number of sub-samples for estimation, follow these steps:
 - (i) Choose a sample size from 1b. In our experiments we started with either 10 or 20 and increased by one each cycle.
 - (ii) Estimate the σ using the first table where $\mu = 0$.
 - (iii) Check if the estimator has the smallest standard deviation, if yes, choose it and stop. If not, go back to Step 1a and choose another sample size.
 - (iv) Repeat steps 1(c)i-1(c)iii until the estimator with the smallest standard deviation is found.
2. In case estimating the κ :
 - (a) We have expanded the procedure for the Independent Approximate Subsamples (IAs) from pairs to triplets. The samples are randomly partitioned into $\lfloor N/3 \rfloor$ triplets, represented as $(X_{i_1}, X_{i_2}, X_{i_3}), (X_{i_4}, X_{i_5}, X_{i_6}), \dots, (X_{i_{N-2}}, X_{i_{N-1}}, X_{i_N})$, where i_1, i_2, \dots, i_N is a random permutation of the integers $1, 2, \dots, N$. For each triplet, we calculate the absolute differences $d_I = \max(|X_{i_{3I-2}} - X_{i_{3I-1}}|, |X_{i_{3I-1}} - X_{i_{3I}}|)$ and retain only those triplets whose maximum difference is less than or equal to the tolerance ϵ . The optimal number of sub-samples can be found using the same step 1c.

The finite $n - 1$ moment occurs when the density function f is raised to the power of n , ensuring that the bias remains finite. In the subsequent analysis, we assume that the subsamples to be independent and identical. To simplify notation, we assume μ as a known constant. Therefore, in proving the asymptotic results for σ and κ , we will utilize the first and second moments, respectively. Let $\mu_m^{(n)}$ represent the general m th moment for a n th power density function. The expressions for the general power moments of the Generalized Pareto Distribution (GPD) are as follows:

$$\mu_m^{(n)} = \left(\frac{\kappa}{\sigma}\right)^{-m} \frac{m! \left(-2 - m + n + \frac{n}{\kappa}\right)!}{\left(-2 + n + \frac{n}{\kappa}\right)!} \quad \text{for } \kappa < \frac{n}{2 + m - n}. \quad (6)$$

Finally, we define $\hat{\sigma}$ as the estimate of the scale parameter and $\hat{\kappa}$ as the estimate of the shape parameter, given by $\hat{\sigma} = 2\hat{\mu}^{(2)}$ and $\hat{\kappa} = \frac{8(\hat{\mu}_1^2)^{(2)}}{3\hat{\mu}_1^{(3)}} - 3$ for coupled exponential and

$\hat{\sigma} = \sqrt{3\mu_2^{(3)}}$ for coupled Gaussian. I^2 and I^3 represent pairs and triplets of independent approximations, respectively. These moment estimates are based on the values presented in (Nelson, 2022, Table 1) and (Nelson, 2022, Table 3). For convenience, we list these tables here, Tables 1, 2.

In this paper we focus on the estimation of the scale and shape assuming the location is known. For the coupled Gaussian estimating three parameters is straightforward since $\mu_1^{(2)}$ and $\mu_2^{(3)}$ are independent of each other. For the coupled exponential distribution, further investigation is required to determine a set of three moments that are sufficiently independent.

Table 1: The n th moments for the $(n + 1)$ -power-density of the one-sided GPD.

Moment, Centered	One side Pareto type II	
	Non centered	Centered (Geometric mean or Log-Average)
$\mu_0, x - \mu$	-	-
$\mu_1^{(2)}, x - \mu$	$\mu + \frac{\sigma}{2}$	$\frac{\sigma}{2}$
$\mu_2^{(3)}, x - \mu$	$\mu^2 + \frac{2\mu\sigma}{3 + \kappa} + \frac{2\sigma^2}{3(3 + \kappa)}$	$\frac{2\sigma^2}{3(3 + \kappa)}$
$\mu_3^{(4)}, x - \mu$	$\mu^3 + \frac{3\mu^2\sigma}{(4 + 2\kappa)} + \frac{12\mu\sigma^2 + 3\sigma^3}{2(4 + \kappa)(4 + 2\kappa)}$	$\frac{3\sigma^3}{2(4 + \kappa)(4 + 2\kappa)}$
$\mu_4^{(5)}, x - \mu$	$\mu^4 + \frac{4\mu^3\sigma}{5 + 3\kappa} + \frac{12\mu^2\sigma^2}{(5 + 2\kappa)(5 + 3\kappa)} + \frac{24\sigma^4}{5(5 + \kappa)(5 + 2\kappa)(5 + 3\kappa)}$	$\frac{120\mu\sigma^3 + 24\sigma^4}{5(5 + \kappa)(5 + 2\kappa)(5 + 3\kappa)}$
$\mu_{(n)}^{(n+1)}, x - \mu$	$\sum_{i=0}^n \frac{n! \mu^{n-i} \sigma^i}{(n-1)!} \frac{1 + n + (n-i-1)\kappa}{(\kappa^i) \frac{1 + n + (n-1)\kappa}{\kappa}}$	$\kappa^{-n} \frac{n! \frac{1 + n - \kappa}{1 + n + n\kappa - \kappa}}{\kappa} \sigma^{-n}$

Table 2: The n th moments for the $(n + 1)$ -power-density the Student's t-distribution.

Moment, Centered	Student's t, n+1	
	Non centered	Centered (Geometric mean or Log-Average)
$\mu_0, x - \mu$	-	-
$\mu_1^{(2)}$	μ	μ
$\mu_2^{(3)}, x - \mu$	$\mu^2 + \frac{\sigma^2}{3}$	$\frac{\sigma^2}{3}$
$\mu_3^{(4)}, x - \mu$	$\mu^3 + \frac{3\mu\sigma^2}{(4 + \kappa)}$	0
$\mu_4^{(5)}, x - \mu$	$\mu^4 + \frac{6\mu^2\sigma^2}{5 + 2\kappa} + \frac{3\sigma^4}{5(5 + 2\kappa)}$	$\frac{3\sigma^4}{25 + 10\kappa}$
$\mu_{(n)}^{(n+1)}, x - \mu$	Simplification Not Available	$(1 + (-1)^n) \left(\frac{\sigma}{\sqrt{\kappa}}\right)^n \frac{\frac{n-1}{2}! \frac{n+1-2\kappa}{2\kappa}}{2\sqrt{\pi} \frac{n+1+(n-2)\kappa}{2\kappa}}$

3.2 Theoretical part

In this section, proves are provided regarding the bias and consistency of estimated parameters, namely σ and κ using IA.

Lemma 3.1. 1. Suppose that the $X_i^{(2)}, i = 1, 2, \dots, N^{(2)}$ is independent-equal samples drawn from a 2-power coupled exponential distribution. The estimates of the scale parameter, $\hat{\sigma}$, is an unbiased estimator of σ .

2. Suppose that the $X_i^{(3)}, i = 1, 2, \dots, N^{(3)}$ samples from a centered 3-power coupled exponential density $f^{(3)}(x)$. The estimates of the scale $\hat{\kappa}$ is a biased estimator of κ .

Proof. The proof follows the general outline of the proof of Lemma 4 Nelson (2022).

1.

$$\begin{aligned} E[2\hat{\mu}_1^{(2)} - \sigma] &= 2E \left[\frac{1}{I^{(2)}} \sum_{i=1}^{I^{(2)}} X_i^{(2)} - \sigma \right] \\ &= \frac{2}{I^{(2)}} \sum_{i=1}^{I^{(2)}} E(X_i^{(2)}) - \sigma \end{aligned}$$

By applying $E(X_i) = \sigma/2$ from Table 1, the proof is completed.

2. Given the unbiased estimate $\hat{\sigma}$, the independence of $\hat{\mu}^{(2)}$ and $\hat{\mu}^{(3)}$, the bias of the estimate $\hat{\kappa}$ is given by

$$\begin{aligned} \frac{2}{3}E \left[\frac{\hat{\sigma}^2}{\hat{\mu}_2^3} - 3 - \kappa \right] &= \frac{2\sigma^2}{3} E \left[\frac{1}{\frac{1}{I^3} \sum_{i=1}^{I^{(3)}} (X_i^{(3)} - \hat{\mu})^2} \right] - 3 - \kappa \\ &= \frac{2\sigma^2}{3} \left[\frac{1}{\frac{2\sigma^2}{3(3+\kappa)} - \frac{2\sigma^2}{3I^{(2)}(3+\kappa)}} \right] - (3 + \kappa) \\ &= \frac{3 + \kappa}{I^{(2)} - 1} \end{aligned}$$

□

Lemma 3.2. 1. Let $\hat{\sigma} = 2\mu_1^{(2)}$ be the estimator of σ based on the independent-equal samples $X_i^{(2)}, i = 1, \dots, N^{(2)}$ with the (p.d.f) of GPD. Then $\hat{\sigma} \xrightarrow{P} \sigma$.

2. Let $\hat{\kappa} = \frac{2\hat{\sigma}^2}{3\hat{\mu}_2^{(3)}} - 3$ be the estimator of κ based on the independent-equal samples $X_i^{(3)}, i = 1, \dots, I^{(3)}$ with the (p.d.f) of GPD. Then $\hat{\kappa} \xrightarrow{P} \kappa$.

Proof. 1. Let $\hat{\theta}_n = \hat{\theta}_n(X_1, \dots, X_n)$ be the estimator of θ based on the random sample X_1, \dots, X_n with p.d.f. $f(x, \theta)$. The proof is based on the following theorem

Theorem 3.3. *An asymptotically unbiased estimator $\hat{\theta}_n$ for θ is a consistent estimator of θ if $\lim_{n \rightarrow \infty} \text{Var}(\hat{\theta}_n) = 0$ as $n \rightarrow \infty$*

According to Theorem 3.3, we have

$$\begin{aligned} \lim_{I^{(2)} \rightarrow \infty} \text{Var}(\hat{\sigma}_I^{(2)}) &= \lim_{I^{(2)} \rightarrow \infty} 4 \text{Var} \left(\frac{1}{I^{(2)}} \sum_{i=1}^{I^{(2)}} X_i^{(2)} \right) \\ &= \lim_{I^{(2)} \rightarrow \infty} \frac{4}{I^{(2)}} \frac{2\sigma^2}{3(3+\kappa)} \\ &= \lim_{I^{(2)} \rightarrow \infty} \frac{8\sigma^2}{3I^{(2)}(3+\kappa)} \end{aligned}$$

The term in the last line tends to zero when $I^{(2)} \rightarrow \infty$, which means that the Variances ($\hat{\sigma}$) have zero limits. The sample Variances is consistent using Theorem 3.3

2. From 2 [Lemma 2.1], $\hat{\kappa}$ is a biased estimator for κ . However, because $1 - \frac{1}{I^{(2)}} \rightarrow 1$ as $I^{(2)} \rightarrow \infty$, we have

$$\lim_{I \rightarrow \infty} E(\hat{\kappa}_I) = \lim_{I \rightarrow \infty} \left(\frac{3+\kappa}{1 - \frac{1}{I^{(2)}}} \right) - 3 = \kappa. \quad (7)$$

The κ estimator for the κ parameter is thus asymptotically unbiased.

Using the variance criterion for consistency Theorem 3.3 and under the assumption that the $I^{(2)} > I^{(3)}$, we have

$$\lim_{I \rightarrow \infty} \text{Var}(\hat{\kappa}_I) = \lim_{I \rightarrow \infty} \left(16 \text{Var}(\hat{\mu}^{(2)})^2 \times \left[\frac{1}{\frac{9}{I^{(3)^2}} \sum_{i=1}^{I^{(3)}} (\text{Var}(x_i^{(3)})^2 + \text{Var}(\hat{\mu}^2))} \right] \right)$$

The variance of the square of the samples from a 3-power coupled exponential density is given by $m = 4, n = 3$ in 6

$$\begin{aligned} \frac{\int_{-\infty}^{\infty} x^4 f^3(x) dx}{\int_{-\infty}^{\infty} f^3(x) dx} &= \left(\frac{\kappa}{\sigma} \right)^{-4} \frac{4! \left(-2 - 4 + 3 + \frac{3}{\kappa} \right)!}{\left(-2 + 3 + \frac{3}{\kappa} \right)!} \\ &= \frac{8\sigma^4}{(-3 + \kappa)(3 + \kappa)(-3 + 2\kappa)} \end{aligned}$$

The variance of the 2-power samples is given by $m = 2, n = 2$

$$\text{Var}(\hat{\mu}) = \frac{\sigma^2}{I^{(2)}(2 - \kappa)}, \quad \kappa < 2$$

The variance of the square of the location estimate is the square of the variance of the location estimate. Thus,

$$\begin{aligned} \lim_{I \rightarrow \infty} \text{Var}(\hat{\kappa}_I) &= \lim_{I^{(2)} \rightarrow \infty} \left[\frac{2}{\frac{9(I^{(2)}(2-\kappa))^2}{I^{(3)}} \times \left(\frac{1}{(-3+\kappa)(3+\kappa)(-3+2\kappa)} + \frac{2}{(I^{(2)}(2-\kappa))^2} \right)} \right] \\ &= 0 \end{aligned}$$

Thus from 7 and variance criterion, the variance of the 2-power samples from a GPD is consistent with κ . □

4 Analysis of Performance and Applications

4.1 Simulation results

In this section, we present a comprehensive evaluation of the performance of the Independent Approximates (IA) algorithm by conducting a simulation study using samples drawn from a known distribution. Our main goal is to conduct a robust empirical comparison between our method and the conventional Maximum Likelihood (ML) approach for estimation of heavy-tailed distributions, particularly the coupled exponential and coupled Gaussian. In the study, samples from a coupled exponential distribution (generalized Pareto) are drawn using (2) with α set to 1. Samples from a coupled Gaussian (Student's t) are drawn using the generalized Box-Müller method [Thistleton et al. \(2007\)](#); [Nelson and Thistleton \(2021\)](#). To assess the effectiveness and accuracy of our algorithm, we employ a range of evaluation criteria, including the Coefficient of Efficiency (CE), Average Deviation (AD), Cramer-von Mises (CvM), and Negative Log-Likelihood (NLL). These criteria serve as reliable indicators to gauge the performance of our approach across different scenarios.

For the IA estimate of the scale and shape parameters for one-sided GPD distributions, we compare two approaches. In both cases the IA-pairs mean $\mu_1^{(2)}$ is one of the statistics. This is combined with either the geometric mean of original samples μ_0 or the IA-triplets second-moment $\mu_2^{(3)}$. We conduct parameter estimation for various values of the shape parameter κ , spanning the range from 0.25 to 2, and for the sample size of $N = 10,000$. Performance for samples sizes of 100 and 1000 are provided in [Appendix B](#).

To ensure the accuracy of our estimation, we develop an optimal subsampling technique aimed at minimizing estimation errors. This technique involves selecting the optimal subsample by minimizing the least absolute deviation (LAD) of the estimate,

either $\mu_1^{(2)}$ or $\mu_2^{(3)}$, for selecting pairs and triplets, respectively. To find the optimal configuration, we employ a search method that varies the number of subsamples until the optimal outcome is achieved. The LAD method for determining the optimal subsample of heavy-tailed distributions offers several notable advantages. Heavy-tailed distributions often exhibit outliers or extreme observations, which can substantially impact the accuracy of the estimation process. Unlike traditional mean-based estimators that are sensitive to outliers, the LAD method is known for its robustness and resilience to extreme values. The LAD method aims to minimize the sum of the absolute deviations between the observed data points and the estimated values. The LAD method, therefore, gives more weight to outliers and extreme observations in the data, as it directly considers their absolute distances from the estimated values. Moreover, the LAD method aligns naturally with the underlying assumption of the generalized Pareto distribution (GPD), which serves as a model for heavy-tailed data. The GPD is designed to capture the tail behaviour of distributions, precisely the region where the LAD method thrives.

Tables 3 and 4 provide a comprehensive analysis of the empirical mean square errors (MSE) and the performance metrics for different estimation methods applied to coupled Gaussian distribution. Specifically, Table 3 details the empirical MSE for the shape κ and scale σ estimations, across various values of κ .

Table 3: Empirical mean square errors (MSE) of parameter estimates for data generated from a coupled Gaussian distribution and for sample size $n = 10,000$. The scale is $\sigma = 0.5$ and the shape κ varies as indicated.

κ	MSE			
	IA_GM		ML	
	$\hat{\kappa}$	$\hat{\sigma}$	$\hat{\kappa}$	$\hat{\sigma}$
0.25	0.080 ± 0.005	0.013 ± 0.003	0.008 ± 0.007	0.006 ± 0.005
0.5	0.006 ± 0.003	0.012 ± 0.003	0.007 ± 0.004	0.007 ± 0.006
1	0.034 ± 0.009	0.005 ± 0.009	0.01 ± 0.01	0.009 ± 0.003
1.25	0.03 ± 0.01	0.001 ± 0.003	0.008 ± 0.009	0.009 ± 0.004
2	0.06 ± 0.02	0.040 ± 0.003	0.01 ± 0.02	0.013 ± 0.007

Table 4 presents insights into the performance of estimation methods for the coupled Gaussian distribution using Average Deviation (AD), Cramer–von Mises (CvM), and Negative Log-Likelihood (NLL) as criteria. The IA_GM method exhibits a distinct performance when compared to the quality metrics used. It appears to be more stable and capable of achieving a better fit with the data in general. This is particularly noticeable in the AD method, where the IA_GM estimator performs significantly better than the ML estimator, especially when κ is high.

In the context of the coupled exponential distribution, Table 5 provides the empirical MSE for the shape κ and scale σ parameters. Our analysis encompassed the IA_GM, IA, and ML methods. The results indicate that the IA_GM and IA methods exhibit superior performance compared to the ML method.

Table 4: Goodness-of-Fit Metrics for the Coupled Gaussian Distribution under Various Methods and Shape Parameters κ with a Fixed Scale Parameter ($\sigma = 0.5$).

Coupled Gaussian					
Average deviation (AD) $\sigma = 0.5$					
Method\(κ	0.25	0.5	1	1.25	2
IA (Geometric mean)	0.03	0.063	0.71	4.3	2200
ML	0.034	0.097	17	300	620,000
Cramer-von Mises (CvM) $\sigma = 0.5$					
Method\(κ	0.25	0.5	1	1.25	2
IA (Geometric mean)	0.76	0.75	0.74	0.74	0.79
ML	1.1	1.1	1.0	1.0	0.96
NLL					
Method\(κ	0.25	0.5	1	1.25	2
IA (Geometric mean)	16,000	16,000	19,000	22,000	38,000
ML	17,000	15,000	19,000	22,000	39,000

Table 5: Empirical mean square errors (MSE) of parameter estimates for data generated from a coupled exponential distribution with a sample size $n = 10,000$. The scale $\sigma = 0.5$ and the shape κ varies as indicated.

κ	$(MSE \pm SD) \times 10^{-3}$					
	IA_GM		IA		ML	
	$\hat{\kappa}$	$\hat{\sigma}$	$\hat{\kappa}$	$\hat{\sigma}$	$\hat{\kappa}$	$\hat{\sigma}$
0.25	0 ± 1	1.0 ± 0.1	6 ± 6	9 ± 4	22 ± 5	6 ± 5
0.5	0 ± 5	1.0 ± 0.2	0 ± 4	0 ± 3	20 ± 7	4 ± 5
1	0 ± 10	1.0 ± 0.2	20 ± 10	32 ± 3	20 ± 10	4 ± 5
1.25	3 ± 10	1.0 ± 0.2	3 ± 9	15 ± 4	20 ± 10	3 ± 3
2	20 ± 20	5.0 ± 0.2	60 ± 10	39 ± 6	10 ± 20	13 ± 2

The performance of various estimation methods for the coupled exponential distribution is elucidated in Table 6 using AD, CvM, and NLL as criteria. Notably, in terms of methodological efficacy, exemplary results are observed. For instance, at $\kappa = 0.25$, the IA_GM and IA methods exhibit notably smaller AD values, indicating their superior goodness of fit. This trend persists as κ increases, with IA_GM and IA consistently outperforming ML in the Cramer-von Mises (CvM) tests. These results highlight the robustness of IA_GM and IA in capturing the nuances of the coupled exponential distribution. In contrast, the ML method tends to underperform across the range of κ values, underscoring its limitations in accurately capturing the characteristics of the distribution.

4.2 Analysis of Coherent Noise Model (CNM) Results

To evaluate the effectiveness of the IA estimator with samples from a coupled exponential distribution with unknown parameters, we've utilized data from a simulation of CNM [Celikoglu et al. \(2010\)](#). This model is designed to provide a structured framework for the evaluation of a system's response to external stressors [Newman and Sneppen](#)

Table 6: Goodness-of-Fit Metrics for the Coupled Exponential Distribution under Various Methods and Shape Parameters κ with a Fixed Scale Parameter ($\sigma = 0.5$)

Coupled Exponential					
Average deviation (AD) sigma=0.5					
Method\kappa	0.25	0.5	1	1.25	2
IA (Geometric mean)	0.14x10 ⁻³	0.53x10 ⁻³	0.003	0.17	320
IA (Triplets)	0.007	0.002	0.15	0.14	650
ML	0.013	0.027	0.33	1.57	180
Cramer-von Mises (CvM) Sigma=0.5					
Method\kappa	0.25	0.5	1	1.25	2
IA (Geometric mean)	0.045x10 ⁻³	0.086x10 ⁻³	0.0002	0.001	0.007
IA (Triplets)	0.063	0.0005	0.55	0.11	0.27
ML	0.013	0.009	0.01	0.011	0.078
NLL					
Method\kappa	0.25	0.5	1	1.25	2
IA (Geometric mean)	5,500	8,000	13,000	15,000	23,000
IA (Triplets)	5,500	8,000	13,000	16,000	23,000
ML	5,600	8,100	13,000	16,000	23,000

(1996), Sneppen and Newman (1997). The model involves a collection of N agents, each distinguished by a unique threshold denoted as x_i . These thresholds serve as indicators of the agents' capacity to withstand external stress, represented by the variable η . Importantly, both the threshold values and external stress factors are drawn from probability distributions, namely $p_{threshold}(x)$ and $p_{stress}(\eta)$. The stress is modeled as an exponential distribution $p_{stress}(\eta) = (1/\eta) \exp(-\eta/\sigma)$. The threshold is modeled as a uniform distribution between 0 to 1, $p_{threshold}(x)$:

$$p_{threshold}(x) = \begin{cases} 1 & \text{if } 0 \leq x \leq 1, \\ 0 & \text{otherwise} \end{cases} .$$

We used $\sigma = 0.05$, $f = 8000$ and a time series of 4×10^8 sampled in $N = 10,000$ increments.

The dynamics of the model is very simple, yet effective (for the details of the model, see Wilke et al. (1998), Sarlis and Christopoulos (2012)):

- A random stress factor, η , is generated in accordance with the $p_{stress}(\eta)$ distribution. Agents with threshold values (x_i) falling below η are systematically replaced by new agents, each of whom is endowed with a threshold drawn from the $p_{threshold}(x)$ distribution.
- To maintain the continuity of avalanche generation, a fraction of the N agents, denoted as f , undergo threshold updates. New threshold values for these selected agents are drawn once again from the $p_{threshold}(x)$ distribution.
- This process iterates, with the first step being executed in each subsequent time interval.

Tables 7 and Figure 1a present the parameter estimates and the performance evaluation of estimation methods, utilizing AD, CvM, and NLL as criteria for a Coherent

Noise Model (CNM) based on a coupled exponential distribution. In all three criteria, we note that the IA_GM estimator has better performance than ML and IA. Therefore, based on the provided results, IA_GM appears to be the best method for estimating the coupled exponential distribution for the CNM.

Table 7: Comparison of CNM Parameter Estimates using three methods: ML, IA_GM, and IA

Analyzing Standard Map set Results using a coupled exponential				
Method	$\hat{\kappa}$	$\hat{\sigma}(10^{-3})$	\hat{q}	$\hat{\beta}$
<i>ML</i>	0.961 ± 0.004	4.60 ± 0.001	1.49	4300
<i>IA_GM</i>	0.92 ± 0.05	4.9 ± 0.02	1.5	3900
<i>IA</i>	0.97 ± 0.01	4.90 ± 0.06	1.5	4000

Fig. 1: (a) Evaluation Criteria for Goodness-of-Fit across Three Methods (ML, IA_GM, and IA) in the Coupled Exponential Distribution: The evaluation employs various approaches: AD, CvM, and NLL for the CNM model. (b) Histogram of the Estimated PDF for the Coupled Exponential Distribution: The figure displays the original CNM model along with the estimations using the IA, GM, and ML methods.

Analyzing Coherent Noise Model (CNM) Results using a coupled exponential			
Methods/ Criteria	AD	CvM	NLL
ML	0.005	0.70	60,000
<i>IA_GM</i>	0.001	0.68	60,000
IA	0.001	1.1	60,000

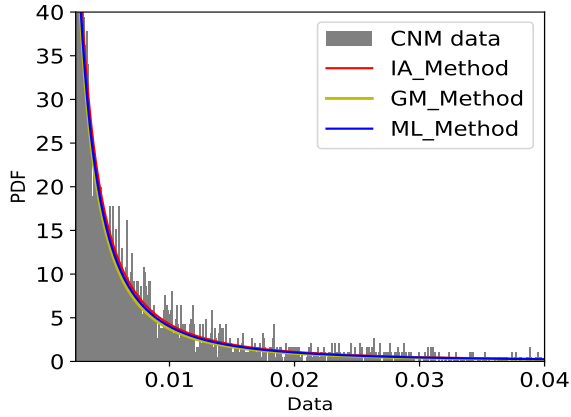
(a)

4.3 The standard map model

To assess the performance of the IA estimator with samples from a coupled Gaussian distribution with unknown parameters we utilized a simulation of the standard map. It is a well-known two-dimensional conservative nonlinear dynamical system described by an iterative function of two variables

$$\begin{aligned} y_{i+1} &= p_i - K \sin(x_i) \\ x_{i+1} &= x_i + y_{i+1} \end{aligned} \tag{8}$$

where x and y are taken as modulo 2π [Zaslavsky \(2005\)](#); [Izraelev \(1980\)](#); [Chirikov \(1979\)](#). It has already been numerically shown [Tirnakli and Borges \(2016\)](#) that, for small K values (for which the phase space is dominated by the stability islands), central limit behavior of the model can be well approximated by a q -Gaussian with



(b)

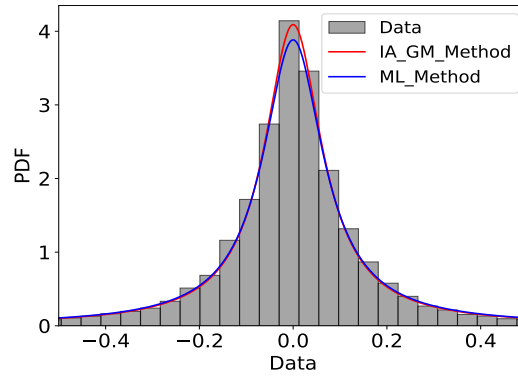
$q \simeq 0.935$, defining the shape based on its relationship with the Tsallis parameter outlined in Section 2. For more details refer to Nelson (2022).

Figure 2a provides a comprehensive comparison of parameter estimates for κ and σ using the IA_GM and ML methods, along with an evaluation of their performance based on the criteria AD, CvM, and NLL. The AD performance of IA_GM excels indicating a superior fit. CvM values further support this trend, with IA_GM presenting a lower CvM value, suggesting a better overall fit. Additionally, NLL values corroborate the superiority of IA_GM, as it achieves a lower NLL value. Based on these criteria, the IA_GM method stands out as a more effective choice compared to the ML method for the specified Standard Map Set with a coupled Gaussian distribution.

Fig. 2: (a) Comparison of Standard Map Parameter Estimates and Evaluation Criteria for Goodness-of-Fit across two Methods (ML, IA_GM) in the Coupled Gaussian Distribution Using Various Approaches (AD, CvM, and NLL for the Map Model). (b) Histogram of the Estimated PDF for the Coupled Gaussian Distribution. The Figure displays the original map data along with the estimations using the Independent Approximates algorithm (IA) and the Maximum Likelihood (ML) method.

Analyzing Standard Map set Results using a coupled Gaussian							
Method	$\hat{\kappa}$	$\hat{\sigma}$	\hat{q}	$\hat{\beta}$	AD	CvM	NLL
<i>IA_GM</i>	0.91 ± 0.05	0.076 ± 0.001	1.953	159	0.43	11	9900
<i>ML</i>	0.900 ± 0.007	0.080 ± 0.001	1.947	146	1.6	12	10,000

(a)



(b)

Acknowledgements

U.T. is a member of the Science Academy, Bilim Akademisi, Turkey and acknowledges partial support from TUBITAK (Turkish Agency) under the Research Project number 121F269. We thank Christian Beck and Grzegorz Wilk for correspondence on the derivation of superstatistics.

References

- Beck, C., Cohen, E.G.D.: Superstatistics. *Physica A: Statistical Mechanics and its Applications* **322**, 267–275 (2003) [https://doi.org/10.1016/S0378-4371\(03\)00019-0](https://doi.org/10.1016/S0378-4371(03)00019-0) . Accessed 2024-04-12
- Bradley, B.O., Taqqu, M.S.: Financial risk and heavy tails. In: *Handbook of Heavy Tailed Distributions in Finance*, pp. 35–103. Elsevier, ??? (2003). <https://www.sciencedirect.com/science/article/pii/B9780444508966500042> Accessed 2024-06-03
- Chirikov, B.V.: A universal instability of many-dimensional oscillator systems. *Physics reports* **52**(5), 263–379 (1979). Publisher: Elsevier. Accessed 2024-06-25
- Celikoglu, A., Tirnakli, U., Queirós, S.M.D.: Analysis of return distributions in the coherent noise model. *Physical Review E* **82**(2), 021124 (2010) <https://doi.org/10.1103/PhysRevE.82.021124> . Publisher: American Physical Society. Accessed 2023-12-30
- Ibragimov, M., Ibragimov, R., Walden, J.: *Heavy-Tailed Distributions and Robustness in Economics And Finance*. Lecture Notes in Statistics, vol. 214. Springer, Cham (2015). <https://doi.org/10.1007/978-3-319-16877-7> . <https://link.springer.com/10.1007/978-3-319-16877-7> Accessed 2024-06-03
- Izraelev, F.M.: Nearly linear mappings and their applications. *Physica D: Nonlinear*

- Phenomena **1**(3), 243–266 (1980). Publisher: Elsevier. Accessed 2024-06-25
- Merz, B., Basso, S., Fischer, S., Lun, D., Blöschl, G., Merz, R., Guse, B., Viglione, A., Vorogushyn, S., Macdonald, E., Wietzke, L., Schumann, A.: Understanding Heavy Tails of Flood Peak Distributions. *Water Resources Research* **58**(6), 2021–030506 (2022) <https://doi.org/10.1029/2021WR030506> . Accessed 2024-06-03
- Nelson, K.P.: Independent Approximates enable closed-form estimation of heavy-tailed distributions. *Physica A: Statistical Mechanics and its Applications* **601**, 127574 (2022) <https://doi.org/10.1016/j.physa.2022.127574> . Accessed 2023-07-22
- Nelson, K.P.: Open Problems within Nonextensive Statistical Mechanics. *Entropy* **26**(2), 118 (2024) <https://doi.org/10.3390/e26020118> . Number: 2 Publisher: Multidisciplinary Digital Publishing Institute. Accessed 2024-03-19
- Newman, M.E.J., Sneppen, K.: Avalanches, scaling, and coherent noise. *Physical Review E* **54**(6), 6226–6231 (1996) <https://doi.org/10.1103/PhysRevE.54.6226> . Accessed 2024-06-25
- Nelson, K.P., Thistleton, W.J.: Comments on “Generalized Box-Müller Method for Generating q-Gaussian Random Deviates”. *IEEE Transactions on Information Theory* **67**(10), 6785–6789 (2021) <https://doi.org/10.1109/TIT.2021.3071489> . Conference Name: IEEE Transactions on Information Theory
- Nelson, K.P., Umarov, S.R., Kon, M.A.: On the average uncertainty for systems with nonlinear coupling. *Physica A: Statistical Mechanics and its Applications* **468**, 30–43 (2017) <https://doi.org/10.1016/j.physa.2016.09.046> . Publisher: Elsevier B.V.
- Resnick, S.: *Heavy-Tail Phenomena: Probabilistic and Statistical Modeling*. Springer, New York, NY (2007). <https://doi.org/10.1007/978-0-387-45024-7> . Series Title: Springer Series in Operations Research and Financial Engineering. <http://link.springer.com/10.1007/978-0-387-45024-7> Accessed 2020-10-24
- Sarlis, N.V., Christopoulos, S.-R.G.: Predictability of the coherent-noise model and its applications. *Physical Review E* **85**(5), 051136 (2012) <https://doi.org/10.1103/PhysRevE.85.051136> . Accessed 2024-06-25
- Shalizi, C.R.: Maximum Likelihood Estimation for q-Exponential (Tsallis) Distributions. arXiv:math/0701854 [math.ST] (2007) <https://doi.org/10.48550/arXiv.math/0701854> . arXiv:math/0701854. Accessed 2023-05-05
- Sneppen, K., Newman, M.E.: Coherent noise, scale invariance and intermittency in large systems. *Physica D: Nonlinear Phenomena* **110**(3-4), 209–222 (1997). Accessed 2024-01-18
- Tirnakli, U., Borges, E.P.: The standard map: From Boltzmann-Gibbs statistics to Tsallis statistics. *Scientific Reports* **6**(1), 23644 (2016) <https://doi.org/10.1038/>

srep23644 . Publisher: Nature Publishing Group. Accessed 2024-06-28

Thistleton, W.J., Marsh, J.A., Nelson, K., Tsallis, C.: Generalized Box–Müller Method for Generating q -Gaussian Random Deviates. *IEEE Transactions on Information Theory* **53**(12), 4805–4810 (2007) <https://doi.org/10.1109/TIT.2007.909173> . Conference Name: IEEE Transactions on Information Theory

Tsallis, C.: On the foundations of statistical mechanics. *The European Physical Journal Special Topics* **226**(7), 1433–1443 (2017) <https://doi.org/10.1140/epjst/e2016-60252-2> . Publisher: Springer. Accessed 2020-07-18

Umarov, S., Tsallis, C.: The limit distribution in the q -CLT for $q \geq 1$ is unique and can not have a compact support. *Journal of Physics A: Mathematical and Theoretical* **49**(41), 415204 (2016) <https://doi.org/10.1088/1751-8113/49/41/415204> . Accessed 2023-12-23

Umarov, S., Tsallis, C., Steinberg, S.: On a q -Central Limit Theorem Consistent with Nonextensive Statistical Mechanics. *Milan Journal of Mathematics* **76**(1), 307–328 (2008) <https://doi.org/10.1007/s00032-008-0087-y> . Accessed 2023-12-23

Wilke, C., Altmeyer, S., Martinetz, T.: Aftershocks in coherent-noise models. *Physica D: Nonlinear Phenomena* **120**(3-4), 401–417 (1998). Publisher: Elsevier. Accessed 2024-06-25

Wilk, G., Włodarczyk, Z.: Interpretation of the Nonextensivity Parameter q in Some Applications of Tsallis Statistics and Lévy Distributions. *Physical Review Letters* **84**(13), 2770–2773 (2000) <https://doi.org/10.1103/PhysRevLett.84.2770> . Publisher: APS. Accessed 2015-09-15

Zaslavsky, G.M.: *Hamiltonian Chaos and Fractional Dynamics*. Oxford University Press, New York, NY, USA (2005)

Appendix A Comparison of the coupled and q -distributions

The field of nonextensive statistical mechanics grew out of analysis of complex systems defined by an escort probability $p_i^{(q)} \equiv \frac{p_i^q}{\sum_{j=1}^N p_j^q}$; however, the choice of q as a defining parameter created difficulties in a) relating results to established principles within the statistical analysis of scale-shape distributions, and b) explaining physical theories of complex systems, whose principle property is nonlinear dynamics. Recasting results in nonextensive statistical mechanics, such as this contribution regarding estimation using Independent Approximates, has the potential to integrate advances in modeling complex systems into more establish approaches of statistical analysis and to clarify physical implications. In this appendix, we show that the scale-shape definition of the coupled distributions provides clear mathematical properties which are obscured when using the β - q translation.

Table A1: Comparison of mathematical properties of the Coupled Gaussian and q -Gaussian representations. The results are for the heavy-tailed domain in which $0 < \kappa < \infty$ and $1 < q < 3$.

Property	Mathematical Description	Coupled Gaussian	q -Gaussian
Inflection Point	$f''(x) = 0$	$x = \frac{\pm\sigma}{\sqrt{1+2\kappa}}$	$x = \frac{\pm 1}{\sqrt{\beta(q+1)}}$
Inflection of Derivative	$f^{(3)}(x) = 0$	$x = \frac{\pm\sigma\sqrt{3}}{\sqrt{1+2\kappa}}$	$x = \frac{\pm\sqrt{3}}{\sqrt{\beta(q+1)}}$
Half asymptotic slope of Log-Log plot	$x = e^u$ $g'(u) = \frac{e^u f'(e^u)}{f(e^u)} = \frac{1}{2} \lim_{u \rightarrow \infty} g'(u)$	$x = \frac{\sigma}{\sqrt{\kappa}}$	$x = \sqrt{\frac{1}{\beta(q-1)}}$
Log-Log Derivative is -1	$x = e^u$ $g'(u) = -1$	$x = \sigma$	$x = \sqrt{\frac{1}{\beta(3-q)}}$

Table A1 shows a comparison of basic mathematical properties of the coupled Gaussian and q -Gaussian distributions. The inflection point of the pdf and its derivative have comparable complexity with the coupled and q -Gaussian representations. However, key points of the Log-Log plot of the pdfs show a simplification for the coupled Gaussian. The point at which the slope of the log-log plot equals -1 is always the scale of the distribution, $x = \sigma$. The translation to the q -Gaussian does not have this clarity, $x = \sqrt{\frac{1}{\beta(3-q)}}$. Likewise, the point at which the log-log slope is half the slope at the asymptotic limit is simply, $|x| = \frac{\sigma}{\sqrt{\kappa}}$; whereas, the q -Gaussian has the -1 constant which complicates interpretation, $|x| = \sqrt{\frac{1}{\beta(q-1)}}$.

The significance of the scale for properties of nonadditive entropy was introduced in Nelson et al. (2017) and discussed further in Nelson (2024). For the coupled distributions the density at the scale is equal to an average density defined by the translation

of the coupled entropy from the log-density domain back to the density domain. That is, for the coupled exponential ($\alpha = 1$) and the coupled Gaussian ($\alpha = 2$) (2) the density at the scale is equal to the following generalized mean of the distribution

$$f(\sigma; \kappa, \alpha) = \left(\int_{x \in X} f(x; \kappa, \alpha)^{1 + \frac{\alpha \kappa}{1 + \kappa}} dx \right)^{\frac{1 + \kappa}{\alpha \kappa}}. \quad (\text{A1})$$

Given the mathematical significance of the coupled distributions at the scale, the physical interpretation of heavy-tailed phenomena should also simplify with this representation.

The difficulty in interpreting q -statistics is illustrated by the interpretations of superstatistics by Beck and Cohen [Beck and Cohen \(2003\)](#), and Wilk and Włodarczyk [Wilk and Włodarczyk \(2000\)](#). Solving for a generalization of the Boltzmann factor and then normalizing the solution, these investigators concluded that a random variable with a fluctuating standard deviation can be modeled as q -exponential distribution with q proportional to the relative variance. The q -exponential distribution is exact if the variations β are distributed as a gamma distribution. Furthermore, via Taylor series analysis this result is shown to be universal for small fluctuations regardless of the large-scale distribution of the fluctuations.

However, examination of the result reveals a couple of problems. First, the relative variance has a domain from 0 to infinity while the heavy-tailed q -exponentials can only be normalized from $1 < q < 2$. Secondly, the superstatistics derivation utilized the Boltzmann factor $e^{-\beta E}$ which neglects the normalization. These issues led to the definition of Type B superstatistics, in which the variation in the normalization is included. While the result is still a q or coupled exponential distribution, the relative variance is now equal to the coupling κ , which like the relative variance has domain over the positive reals for heavy-tailed distributions.

Anticipating the coupled exponential distribution solution we use σ' as the variable scale and the following parameters for the mean and relative variance of the inverse scale:

$$\frac{1}{\sigma} = \left\langle \frac{1}{\sigma'} \right\rangle, \quad \kappa = \frac{\left\langle \frac{1}{\sigma'^2} \right\rangle - \left\langle \frac{1}{\sigma'} \right\rangle^2}{\left\langle \frac{1}{\sigma'} \right\rangle^2}. \quad (\text{A2})$$

With the normalization treated as a constant, the Type A superstatistics result is

$$C \left(1 + \kappa \frac{x}{\sigma} \right)^{-\frac{1}{\kappa}} = C \int_0^\infty e^{-\frac{x}{\sigma'}} \frac{(\sigma \kappa^{-1})^{\frac{1}{\kappa}}}{\Gamma\left(\frac{1}{\kappa}\right)} \left(\frac{1}{\sigma'} \right)^{\frac{1}{\kappa} - 1} e^{-\frac{\sigma}{\kappa} \frac{1}{\sigma'}} d\left(\frac{1}{\sigma'} \right). \quad (\text{A3})$$

From this result, the q -exponential distribution is formed by the substitutions,

$$\kappa = q - 1, \quad \sigma = \frac{1}{\beta}, \quad C = \beta(2 - q), \quad (\text{A4})$$

which provided the interpretation that the relative variance is proportional to q . In contrast, if the normalization of the exponential distribution is included the Type B

superstatistics result is

$$\frac{1}{\sigma} \left(1 + \kappa \frac{x}{\sigma}\right)^{-\left(\frac{1}{\kappa}+1\right)} = \int_0^\infty \frac{1}{\sigma'} e^{-\frac{x}{\sigma'}} \frac{(\sigma \kappa^{-1})^{\frac{1}{\kappa}}}{\Gamma\left(\frac{1}{\kappa}\right)} \left(\frac{1}{\sigma'}\right)^{\frac{1}{\kappa}-1} e^{-\frac{\sigma}{\kappa} \frac{1}{\sigma'}} d\left(\frac{1}{\sigma'}\right). \quad (\text{A5})$$

Now, the result is precisely the normalized coupled exponential distribution and the relative variance is equal to the coupling. The translation to q using (4) is $\kappa = \frac{q-1}{2-q}$. While there may be some applications of Type A superstatistics relevant to generalizations of the Boltzmann factor, it cannot be used to derive a distribution in which the variation of the normalization was neglected.

Appendix B

Table B2: Empirical mean square errors (MSE) of parameter estimates for data generated from a Coupled Gaussian distribution with a sample size $n = 1000$. The scale $\sigma = 0.5$ and the shape κ varies as indicated.

κ	$(MSE \pm SD) \times 10^{-3}$			
	IA_GM		ML	
	$\hat{\kappa}$	$\hat{\sigma}$	$\hat{\kappa}$	$\hat{\sigma}$
0.25	71 ± 5	8 ± 2	19 ± 3	17 ± 3
0.5	30 ± 10	5 ± 3	3 ± 6	12 ± 3
1	20 ± 20	8 ± 4	10 ± 8	10 ± 4
1.25	10 ± 20	21 ± 5	10 ± 10	11 ± 3
2	49 ± 25	41 ± 6	20 ± 10	13 ± 3

Table B3: Goodness-of-Fit Metrics for the Coupled Gaussian Distribution under Various Methods and Shape Parameters κ with a Fixed Scale Parameter ($\sigma = 0.5$) and sample size= 1000.

Coupled Gaussian					
Average deviation (AD) $\sigma = 0.5$					
Method \ κ	0.25	0.5	1	1.25	2
IA (Geometric mean)	0.067	0.12	0.69	1.7	163
ML	0.051	0.11	0.78	2.61	150
Cramer-von Mises (CvM) $\sigma = 0.5$					
Method \ κ	0.25	0.5	1	1.25	2
IA (Geometric mean)	0.012	0.023	0.025	0.022	0.023
ML	0.13	0.15	0.14	0.13	0.093
NLL					
Method \ κ	0.25	0.5	1	1.25	2
IA (Geometric mean)	1,900	1,500	1,800	2,100	3,800
ML	1,600	1,500	1,800	2,100	3,700

Table B4: Empirical mean square errors (MSE) of parameter estimates for data generated from a Coupled Gaussian distribution with a sample size $n = 100$. The scale $\sigma = 0.5$ and the shape κ varies as indicated.

κ	$(MSE \pm SD) \times 10^{-3}$			
	IA_GM		ML	
	$\hat{\kappa}$	$\hat{\sigma}$	$\hat{\kappa}$	$\hat{\sigma}$
0.25	53 ± 8	81 ± 8	10 ± 9	20 ± 3
0.5	20 ± 10	60 ± 4	20 ± 10	17 ± 3
1	216 ± 9	20 ± 10	60 ± 20	13 ± 3
1.25	450 ± 10	118 ± 2	20 ± 20	10 ± 2
2	150 ± 20	14 ± 3	120 ± 20	62 ± 3

Table B5: Goodness-of-Fit Metrics for the Coupled Gaussian Distribution under Various Methods and Shape Parameters κ with a Fixed Scale Parameter ($\sigma = 0.5$) and sample size = 100.

Coupled Gaussian					
Average deviation (AD) $\sigma = 0.5$					
Method \ κ	0.25	0.5	1	1.25	2
IA (Geometric mean)	0.081	0.19	1.5	2.7	160
ML	0.21	0.45	2.6	7.6	270
Cramer-von Mises (CvM) $\sigma = 0.5$					
Method \ κ	0.25	0.5	1	1.25	2
IA (Geometric mean)	0.23	0.22	0.24	0.20	0.48
ML	0.31	0.30	0.29	0.26	0.38
NLL					
Method \ κ	0.25	0.5	1	1.25	2
IA (Geometric mean)	160	150	210	250	250
ML	180	160	210	240	260

Table B6: Empirical mean square errors (MSE) of parameter estimates for data generated from a Coupled Exponential distribution with a sample size $n = 1000$. The scale $\sigma = 0.5$ and the shape κ varies as indicated.

κ	$(MSE \pm SD) \times 10^{-3}$					
	IA_GM		IA		ML	
	$\hat{\kappa}$	$\hat{\sigma}$	$\hat{\kappa}$	$\hat{\sigma}$	$\hat{\kappa}$	$\hat{\sigma}$
0.25	6±2	1.0±0.1	0±4	1±3	22±4	5±4
0.5	117±5	34.0±0.3	30±3	33±5	20±10	4±3
1	1±2	2.0±0.2	27±20	68±3	20±10	4±5
1.25	30±10	7.0±0.1	9±10	13±4	30±10	3±2
2	80±10	24.0±0.2	10±20	50±10	30±10	2±2

Table B7: Goodness-of-Fit Metrics for the Coupled Exponential Distribution under Various Methods and Shape Parameters κ with a Fixed Scale Parameter ($\sigma = 0.5$) and sample size=1000.

Coupled Exponential					
Average deviation (AD) $\sigma = 0.5$					
Method\ κ	0.25	0.5	1	1.25	2
IA (Geometric mean)	0.004	0.12	0.021	0.79	140
IA (Triplets)	0.002	0.033	0.17	0.16	4.1
ML	0.011	0.023	0.17	0.53	29
Cramer-von Mises (CvM) $\sigma = 0.5$					
Method\ κ	0.25	0.5	1	1.25	2
IA (Geometric mean)	0.0004	0.066	0.0005	0.002	0.016
IA (Triplets)	0.0004	0.13	0.45	0.014	0.13
ML	0.003	0.002	0.002	0.002	0.003
NLL					
Method\ κ	0.25	0.5	1	1.25	2
IA (Geometric mean)	1100	1610	2600	3100	4600
IA (Triplets)	1100	1600	2600	3100	4600
ML	1100	1600	2600	3100	4600

Table B8: Empirical mean square errors (MSE) of parameter estimates for data generated from a Coupled Exponential distribution with a sample size $n = 100$. The scale $\sigma = 0.5$ and the shape κ varies as indicated.

κ	$(MSE \pm SD) \times 10^{-3}$					
	IA_GM		IA		ML	
	$\hat{\kappa}$	$\hat{\sigma}$	$\hat{\kappa}$	$\hat{\sigma}$	$\hat{\kappa}$	$\hat{\sigma}$
0.25	6±3	10±1	114±5	77±3	113±5	20±5
0.5	125±6	20±1	250±10	253±4	121±6	19±4
1	40±30	10±1	50±20	88±2	140±10	16±5
1.25	0±10	32±2	410±10	264±3	10±20	13±2
2	10±20	83±3	30±10	157±5	200±20	27±2

Table B9: Goodness-of-Fit Metrics for the Coupled Exponential Distribution under Various Methods and Shape Parameters κ with a Fixed Scale Parameter ($\sigma = 0.5$) and sample size=100

Coupled Exponential					
Average deviation (AD) $\sigma = 0.5$					
Method\ κ	0.25	0.5	1	1.25	2
IA (Geometric mean)	0.016	0.089	0.18	0.16	4.0
IA (Triplets)	0.040	0.16	0.13	1.3	5.5
ML	0.046	0.087	0.35	0.70	8.6
Cramer-von Mises (CvM) $\sigma = 0.5$					
Method\ κ	0.25	0.5	1	1.25	2
IA (Geometric mean)	0.003	0.036	0.006	0.008	0.018
IA (Triplets)	0.031	0.24	0.036	0.43	0.074
ML	0.005	0.006	0.006	0.007	0.15
NLL					
Method\ κ	0.25	0.5	1	1.25	2
IA (Geometric mean)	49	73	120	140	210
IA (Triplets)	49	75	120	150	150
ML	49	72	120	140	150